Raman Spectroscopy of Folded and Scrolled Graphene

Ramakrishna Podila,[†,‡] Rahul Rao,[§,¶] Ryuichi Tsuchikawa,[⊥] Masa Ishigami,[⊥] and Apparao M. Rao[†,∥,*]

[†]Department of Physics and Astronomy, Clemson University, Clemson, South Carolina 29634, United States, [‡]Department of Pharmacology and Toxicology, Brody School of Medicine, East Carolina University, Greenville, North Carolina 27834, United States, [§]Materials and Manufacturing Directorate, Air Force Research Laboratory, Wright-Patterson Air Force Base, Ohio 45433, United States, [⊥]Department of Physics and Nanoscience Technology Center, University of Central Florida, Orlando, Florida 32816, United States, and [∥]Center for Optical Materials Science and Technology, Clemson University, Clemson, South Carolina 29634, United States. [¶]Present address: Honda Research Institute, Columbus, Ohio 43212.

ABSTRACT

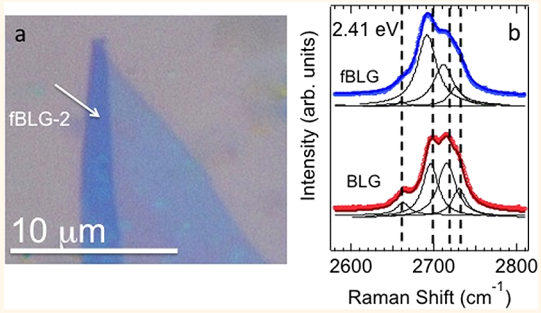

Here we examine the effects of folding and scrolling on the Raman spectra of mechanically exfoliated single- and bilayer graphene prepared on SiO_2 substrates. We find that incommensurate folding in bilayer graphene results in a shift of the second-order G′ band frequency, similar to that observed in folded single-layer graphene due to fold-induced changes in the phonon/electronic energy dispersion. Importantly, we show that the contrasting Raman shifts reported for the G′ band frequency in folded graphene can be rationalized by taking into account the relative strength of fold-induced electron/phonon renormalization. More interestingly, we find that curvature in scrolled graphene lifts the degeneracy of the G band and results in a splitting of the G band and the appearance of low-frequency radial breathing-like (RBLM) modes. This study highlights a variety of Raman signatures for fold-induced and curvature-induced graphene and sets the stage for further theoretical and experimental studies of these novel structures.

KEYWORDS: folded graphene · Raman spectroscopy · Fermi velocity · graphene scrolls

The electronic and vibrational properties of graphene are strongly dependent on its stacking order. While single-layer graphene (SLG) exhibits massless Dirac fermions,[1] misorientation or twist between two or more layers can also result in a similar behavior in the absence of interlayer coupling.[2−4] A change in the electronic structure of misoriented or twisted graphene is evident in their transport[5−7] and spectroscopy measurements.[8−12] Notably, this phenomenon is easy to observe in the Raman spectra of rotationally misoriented graphene layers, which exhibits a blue-shifted and broadened peak in the second-order G′ (also called 2D) band region.[9,10] In addition to misorientation between the individual layers of graphene, the electronic structure of graphene can also be modified by curvature.[13] Such structures of graphene, called scrolled graphene or carbon nanoscrolls, are of interest due to their potential use as nanomechanical actuators[14] and in energy storage.[15] Finally, folding and curvature in multiple graphene layers is also of interest for intercalation and storage due to a large increase in the surface area.[16]

The effects of folding on the Raman spectra of single-layer (also called misoriented/twisted bilayer) graphene have been reported recently by several groups.[9,10,17−19] Blue as well as red shifts of the G′ band frequency due to folding have been observed and accompanied with a broadening of the G′ band. To date, the fundamental origin for these contrasting shifts has been elusive and calls for a detailed re-examination of Raman spectroscopy of folded graphene. To this end, we have collected and analyzed the Raman spectra of folded single- and bilayer graphene (BLG) to elucidate the effects of folding on both the line shape and frequency of the G′ band. As documented in the literature, the G′ band in graphene is well understood within the framework of the double resonance (DR) mechanism, and its profile depends on the phonon and Fermi velocities.[20,21] In this article, we show that the blue or red shift of the G′ band frequency is a direct result of simultaneous changes in the phonon and Fermi velocities and thus resolve the apparent discrepancy in the published literature on Raman spectroscopy of folded graphene. Furthermore, we report the Raman spectrum of scrolled

* Address correspondence to arao@clemson.edu.

Received for review November 7, 2011 and accepted June 27, 2012.

Published online June 27, 2012
10.1021/nn302331p

graphene, wherein a high degree of curvature causes a split in the G band as well as the appearance of low-frequency radial breathing-like (RBLM) modes. Our results highlight Raman signatures for a variety of folded and curvature-induced graphene and serve as the foundation for further theoretical and experimental studies of these novel nanostructures.

RESULTS AND DISCUSSION

The second-order G′ band in SLG arises due to a DR Raman scattering process involving intervalley scattering by two iTO phonons[20,21] (schematic in Figure 1a). This DR process gives rise to an intense peak at ~2700 cm^{-1} (when excited with a visible laser) that can be fit to a single Lorentzian with a typical full width at half-maximum (fwhm) line width of ~25 cm^{-1}.[21] It is important to note that an SLG-like G′ band line shape (only one DR process)[22,23] is also observed in misoriented (non-AB-stacked) or turbostratic graphite due to the absence of the interlayer interaction. However, the G′ band in misoriented, and turbostratic graphite is relatively broader (~45−60 cm^{-1})[22] compared to that of the G′ band in SLG due to symmetry lowering, which relaxes the selection rules for Raman scattering. Figure 1b shows an optical microscope image of SLG where a part of the graphene sheet has folded onto itself. Such folded SLG (fSLG) represents the simplest form of misorientation between two graphene layers, and the absence of AB-stacking between the two layers produces an electronic structure that is similar to that of graphene (*i.e.*, linear bands around the *K*-point of the Brillouin zone), but with a reduced Fermi velocity or a decrease in the slope of the linear energy bands around the *K*-point. This effect is shown schematically with the dotted lines in Figure 1a and was recently verified for twist angles between two graphene layers ranging from 3 to 20°.[7] The reduced Fermi velocity manifests itself in the form of a blue-shifted G′ peak, as seen in the Raman spectra (E_{laser} = 2.33 eV) plotted in Figure 1c. As discussed above, the G′ band in fSLG is relatively broader (fwhm ~45 cm^{-1}) when compared to the G′ band in SLG (fwhm ~25 cm^{-1}). Furthermore, the folding of one graphene layer on itself also causes the appearance of a second peak in the disorder-induced D band region (inset in Figure 1c). In addition to the D band at 1348 cm^{-1}, which is observed in both SLG and fSLG, we observe an additional fold-induced peak at 1358 cm^{-1} in the Raman spectrum of fSLG. This additional peak, which has also been called the I band, is a nondispersive peak that arises due to a weak but well-ordered perturbation caused by the folded layer upon the parent layer.[19,24] The frequency of the I band depends on the fold angle and is ~30° in our sample according to the relation between fold angle and I band frequency reported recently by Carozo *et al.*[25]

In BLG, the interlayer coupling due to AB-stacking leads to a hyperbolic energy dispersion for the two

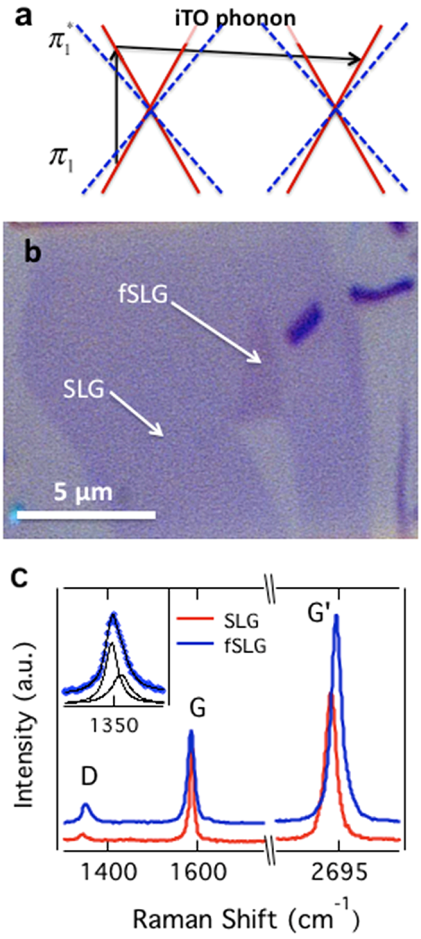

Figure 1. (a) Electronic band structure of SLG near the *K*-point of the graphene Brillouin zone, depicting the intravalley scattering process for the G′ band. Dashed lines signify a Fermi velocity reduction due to folding. (b) Optical microscope image of SLG and fSLG on 300 nm SiO_2/Si substrate. Their corresponding Raman signatures are shown in (c). The inset in (c) shows the two-peak structure of the D band in fSLG.

conduction and valence bands located at the *K*-point (Figure 2a). The DR Raman process involving the electronic bands of BLG is relatively more complex than the Dirac cone in SLG due to the interlayer interaction, which splits the G′ band in BLG into four peaks, P_{22}, P_{21}, P_{12}, and P_{11}.[21] As depicted in Figure 2a, in a process P_{ij} (i, j = 1 or 2), an electron from the ith valence band is excited by an incoming photon at the *K*-point. Subsequently, this excited electron is scattered by an iTO phonon to another electronic state in the jth conduction band (at the *K*′-point). To elucidate the effects of folding on the Raman spectra of BLG, we evaluated three different samples as described below. All three samples were prepared on 300 nm SiO_2/Si to ensure that the observed changes in the G′ band frequency are intrinsic (*i.e.*, fold-induced) and not due to extrinsic factors such as substrate-induced doping of graphene.

Figure 2b shows an optical microscope image of the first folded BLG sample (labeled as fBLG-1 for further discussion) and its corresponding Raman spectrum (E_{laser} = 2.33 eV) in the G′ band region (Figure 2c).

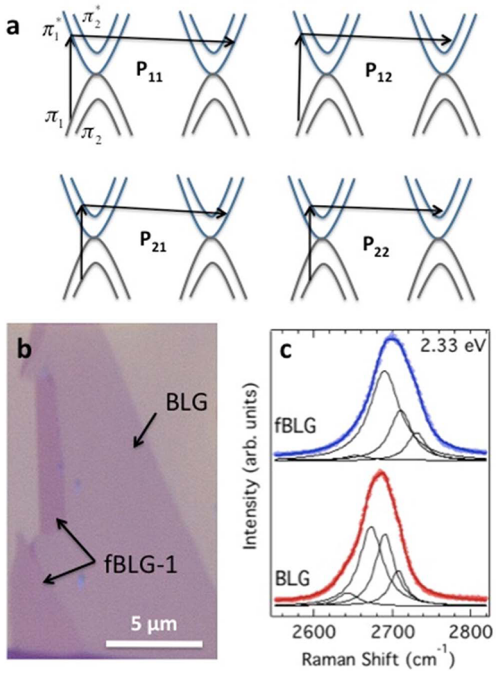

Figure 2. (a) Four scattering processes that contribute to the G′ band intensity in BLG (see text for more details). (b) Optical microscope image of BLG and fBLG on 300 nm SiO_2/Si substrate. Their corresponding Raman signatures in the G′ band region are shown in (c).

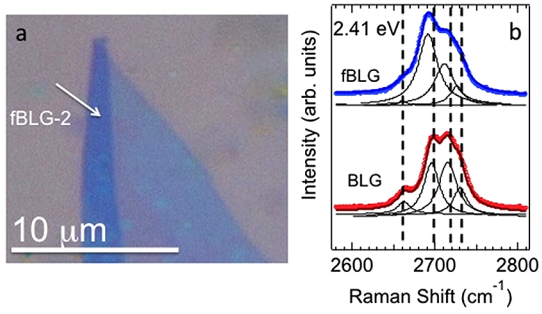

Figure 3. (a) Optical microscope image of BLG and fBLG-2 on 300 nm SiO_2/Si substrate. Their corresponding Raman signatures in the G′ band region are shown in (b).

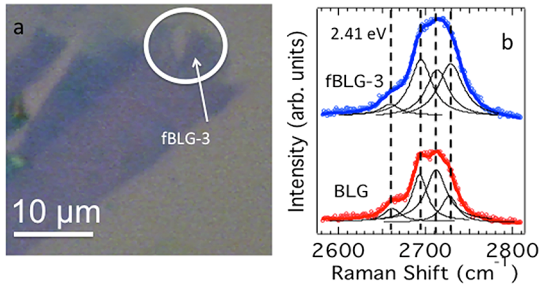

Figure 4. (a) Optical microscope image of BLG and fBLG-3 on 300 nm SiO_2/Si substrate. Their corresponding Raman signatures in the G′ band region are shown in (b).

Following the above description of the four P_{ij} scattering processes, the G′ band in BLG is fitted to four Lorentzians with a fwhm of ~25 cm^{-1}.[21] As seen in Figure 2b, the triangular BLG sample has a folded region along the left vertical edge approximately parallel to the right vertical edge, indicating that the fold angle is low. The low fold angle is also evident in the fact that the G′ band (that is highly sensitive to subtle electronic energy changes) retains the four-peak structure of the parent BLG in the folded region. However, the upshift and broadening of the G′ band in fBLG-1 are indicative of a weak perturbation in the graphene band structure due to folding. Indeed the blue shift of the G′ band in fBLG-1 (~10 cm^{-1}) is very similar to the blue shift due to the reduced Fermi velocity observed in folded SLG (Figure 1c). Moreover, we observe that all of the P_{ij} processes in fBLG-1 upshift and broaden, suggesting that the folding affects the curvature of both the hyperbolic bands equally.[26] Unlike the fold in SLG, we do not observe a separate fold-induced peak in the D band region. In fact, the D band intensity for both BLG and fBLG-1 is negligible, implying that the I band may be a result of a special scattering process between the two misoriented graphene layers in fSLG.

Figure 3a shows an optical microscope image of the second folded BLG (fBLG-2) sample on 300 nm SiO_2. The fold angle in fBLG-2 appears to be higher than that in fBLG-1. Interestingly, we observe a red shift of ~5 cm^{-1} in the G′ band frequency (E_{laser} = 2.41 eV) in fBLG-2 (Figure 3b), which is in contrast to the blue shift observed in fBLG-1 (Figure 2c). It is important to note that the folding in fBLG-2 also leads to a broadening of the G′ band, akin to the broadening observed in fBLG-1. The G′ band of the third folded BLG sample (fBLG-3) shows little or no shift in the G′ band region (Figure 4b), unlike fBLG-1 or fBLG-2. Nevertheless, fBLG-3 also exhibits broadening of the G′ band. In summary, we have observed blue, red, and no shift in the G′ band frequency in fBLG prepared on similar SiO_2 substrates. These results strongly imply that a reduction in Fermi velocity is not the sole reason for the reported shifts in the G′ band frequency in folded graphene and implore a detailed understanding of the fundamental mechanism which leads to a fold-induced blue, red, and no shift in graphene's G′ band frequency.

As explained above, in the DR process for the SLG G′ band, an excited electron with a wave vector k resonantly couples to (two) iTO phonons with $q \approx -2k$ (see Figure 1a). By using the resonant condition (for $q \approx -2k$), the frequency of the G′ band may be written in terms of laser energy (E_{laser}), Fermi and phonon velocities (v_F and v_{iTO}), and iTO frequency at the K-point as follows:

$$\omega_{G'} = AE_{laser} + B$$

$$A = \frac{v_{iTO}}{v_F} \qquad (1)$$

In the above equation, A and B are the ratio of phonon to Fermi velocity and the frequency of the G′ band (or $2\omega_{iTO}$) at the K-point, respectively. The G′ band in SLG disperses with respect to the laser energy according to eq 1, while

the dispersion of the G′ band (P_{ij} processes) in BLG has an additional quadratic component in eq 1.[27] However, the quadratic component in the G′ dispersion for BLG decreases with increasing laser energy. In fact, for laser energies above 1.96 eV, the G′ dispersion in BLG may be explained well in terms of linear phonon dispersion (*cf.* Figure 2a in ref 27). The laser energies used in this study ranged from 1.96 to 2.41 eV, and thus the use of eq 1 to explain the spectral changes in folded BLG is sufficient. In folded graphene, the spectral changes may occur due to the renormalization of *A* or *B*. In view of such renormalization effects, eq 1 may be rewritten as follows for the folded graphene.

$$\begin{aligned}\omega_{G'}^{folded} &= A'E_{laser} + B' \\ \Delta\omega &= \omega_{G'}^{folded} - \omega_{G'} \\ &= (A' - A)E_{laser} + (B' - B)\end{aligned} \quad (2)$$

From eq 2, the slope of $\Delta\omega$ *versus* E_{laser} tracks the fold-induced changes in *A* (or v_{iTO}/v_F). It is important to note that eq 2 has insufficient information for decoupling the effects of changes in the phonon and Fermi velocity. The observed Raman spectral changes are often attributed to a reduction (or increase) in Fermi velocity by assuming that the iTO phonon frequency (*B* in eq 1) remains constant. However, instead of assuming a constant iTO phonon frequency, we can use the intercept of $\omega_{G'}$ *versus* E_{laser} to independently examine the effects of changes in both Fermi velocity and iTO phonon frequency due to folding.

Figure 5 shows the G′ band dispersion for the three fBLG samples as a function of laser energy. Here, we have used the median frequency of the G′ band to indicate the average effect of all P_{ij} processes. The peak frequencies of each of the P_{ij} processes for all of the samples are listed in the Supporting Information. Let us first consider the case of fBLG-1. Recall that the intercept of $\omega_{G'}$ is the G′ band frequency at the *K*-point (or *B* in eq 1). As can be seen in Figure 5a, this intercept is at a lower frequency for the folded region compared to the unfolded region, implying that $B' < B$. This can also be observed in Figure 5b, which plots the difference in G′ band frequencies between the folded and unfolded regions ($\Delta\omega$) against laser energy. The negative intercept of $\Delta\omega$ is another clear indicator of hardening of the iTO phonon branch due to folding and suggests that $B' \leq B$, irrespective of the changes in *A*. In the case of the second folded BLG sample, fBLG-2, the intercept of $\omega_{G'}$ is higher in frequency compared to the unfolded region, implying that $B' > B$. However, the blue shift of the G′ band in the folded region does not remain constant at all laser energies, as can be seen in the inset of Figure 5a. In fact, the G′ band for fBLG-2 is blue-shifted by ~10 cm^{-1} compared the unfolded region at E_{laser} = 1.92 eV, but it is red-shifted by ~5 cm^{-1} at E_{laser} = 2.41 eV (Figure 5b). This difference in shifts suggests that folding in fBLG-2 is more affected by renormalization of the phonon velocity, that is, by

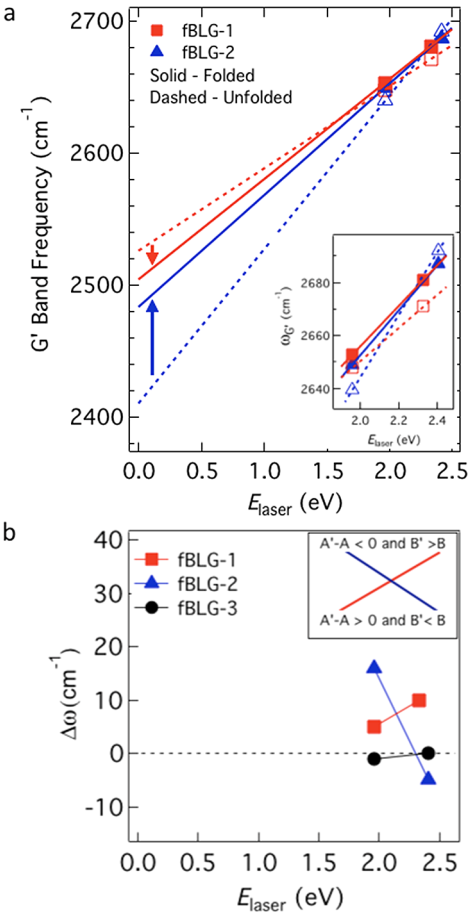

Figure 5. (a) Plot of the G′ band frequencies for the folded (filled data points, solid lines) and unfolded (open data points, dashed lines) BLG samples against laser energy. The inset shows the G′ band dispersion in the narrow energy range used in this study. (b) Plot of $\Delta\omega$ *vs* E_{laser} showing two of the four different cases that may occur upon folding (also see the inset figure). In case 1 (2), shown by red (blue) line, the iTO phonon at the *K*-point softens (hardens). The magnitude of $|B'-B|$ decides the net slope $A'-A$. If $B'-B$ is low (high), then the changes in v_F (v_{iTO}) overwhelm it and result in a corresponding positive or negative slope. The red markers show the experimental values of $\Delta\omega$ for our samples.

changes in the slope *A* (or $A'-A$) rather than due to hardening or softening of the iTO phonon branch at the *K*-point. The third folded BLG region (fBLG-3) exhibits little or no shift compared to the unfolded region, suggesting that for the laser excitations used in this study (1.92 and 2.41 eV) changes in A' and B' balance (or cancel) each other upon folding.

Previously, Maciel *et al.* showed that a defect-induced hardening ($B' \geq B$) or softening ($B' \leq B$) of the G′ band frequency at the *K*-point results in a simultaneous decrease (increase) in v_{iTO} and increase (decrease) in the Fermi velocity.[28] Since all three effects (v_{iTO}, v_F, and *B*) are correlated, the observed changes in the Raman spectra of folded graphene (where the fold is the defect) cannot be solely attributed to renormalization of v_F. That said, the observed changes in our samples fBLG-1, -2, and -3 can be explained by the differences in

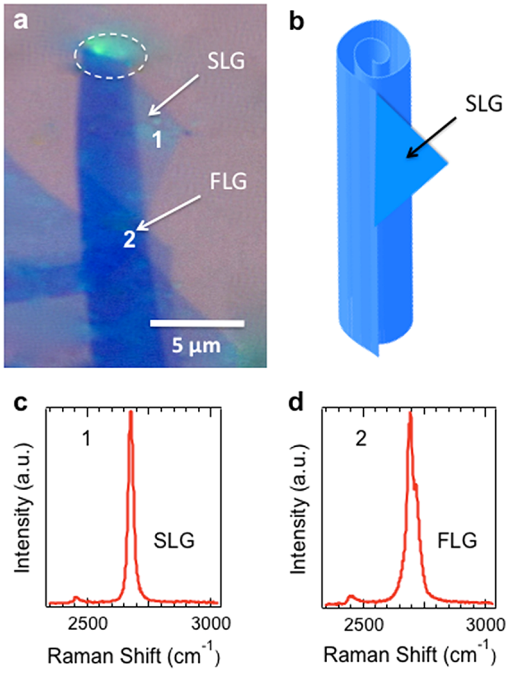

Figure 6. (a) Optical microscope image of scrolled graphene. (b) Magnified three-dimensional schematic of the graphene scroll seen in (a). Panels (c) and (d) depict the Raman spectra in the G′ band region corresponding to the spots indicated in (a).

the value of B' for these samples. Furthermore, we also use this to explain previously observed differences among the Raman spectra of folded graphene (see Figure S1 in Supporting Information).[9,10] At low $|B'-B|$ values, changes in v_F dominate and thus the observed blue shifts in the G′ band frequency upon folding can be explained in terms of Fermi velocity changes (as in the case of Ni *et al.*).[9] In case of higher $|B'-B|$ values, the spectral changes are dictated by renormalization of v_{iTO} leading to a negative slope (as in the case of Poncharal *et al.*).[10] It is worth noting that these intercept changes still hold even with the inclusion of nonlinear effects since B represents the iTO frequency at the K-point.

So far, we have discussed changes in the Raman spectra due to incommensurate folding in SLG and BLG. We now present the curious case of scrolled graphene, where the mechanical exfoliation process can cause the graphene layer to roll up into a scroll, as shown in Figure 6. The formation of such scrolls was completely coincidental. Unfortunately, we could not produce more scrolls akin to Figure 6a. However, we take this opportunity to present the Raman spectrum of scrolled graphene as an extreme case of incommensurate folding. The optical microscope image and a schematic of the graphene scroll are shown in Figure 6a,b, respectively. Interestingly, we observe not only a curvature-induced enhancement of the D band intensity but also a splitting of the G band due to the lifting of degeneracy between longitudinal and transverse optical (LO and TO) phonons. In addition, we also

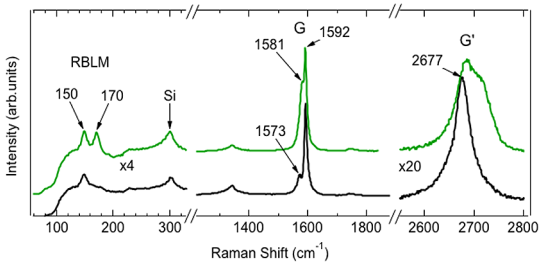

Figure 7. Raman spectra obtained from two different spots near the open end of the graphene scroll shown in Figure 6a.

observe low-frequency radial breathing mode-like (RBLM) modes which strongly suggest that the entity in Figure 6a is a scroll. In Figure 6a, we show a triangular portion of the parent SLG extending beyond the scrolled portion (indicated in the schematic in Figure 6b). The Raman spectrum obtained from this triangle (corresponding to spot 1 in Figure 6a) is shown in Figure 6c. A single Lorentzian peak for the G′ band is observed, confirming that the scroll is formed from a rolled SLG. On the other hand, the spot labeled 2 in Figure 6a exhibits a two-peak G′ band (Figure 6d) and is similar to the two-peak G′ band observed in multilayered graphene and HOPG.[20] This suggests that spot 2 in Figure 6a shows the signature of multiple decoupled graphene layers (FLG), which is a result of scrolling. We note that the G band frequencies at spots 1 and 2 do not vary from the corresponding frequencies in SLG or FLG ($\sim$1580$-$1585 cm^{-1}).

The most remarkable aspect of the scroll is its Raman spectrum from the area indicated by the circle in Figure 6a, which corresponds to the open end of the scroll. Figure 7 shows the low-frequency Raman spectra and the G and G′ band regions from two different spots at the open end of the scroll. It is clear from Figure 7 that the Raman spectrum of scrolled graphene differs significantly from the Raman spectrum of "flat" graphene in several ways: (i) we observe an enhanced D band similar to fSLG due to curvature-induced disorder. This increase in the D band intensity may be attributed to the momentum conservation of the intravalley electrons scattered *via* iTO phonons (at the K-point) by curvature-induced defect scattering. (ii) The curvature present in the scroll lifts the degeneracy between the LO and TO phonons near the Γ-point of the graphene Brillouin zone, leading to a splitting of the G band into additional peaks located at 1570, 1580, and 1592 cm^{-1}. (iii) We see the appearance of low-frequency RBLMs at 150 and 170 cm^{-1}. In fact, the Raman spectra shown in Figure 6 look strikingly similar to that of single-walled carbon nanotubes (SWNTs). Previously, splitting in the G band has been observed in strained graphene samples[29,30] as well as in nanoribbons.[31] Thus the appearance of a D band or splitting of the G band alone cannot confirm the presence of the scroll. However, the RBLMs provide strong support for scrolled graphene. The radial breathing mode

is absent in the Raman spectrum of flat graphene since the low-frequency vibrations correspond to a simple translation of the honeycomb network. However, the curvature in the scroll transforms this translation into a phonon mode similar to the radial breathing mode in SWNTs. It is important to point out that the spectra shown in Figure 7 are only observed from the open end of the scroll and not along the rest of the scroll, suggesting that the edges may play an important role in the activation of RBLMs. We also note that low-frequency RBLMs have been predicted previously in narrow graphene nanoribbons.[32−34] However, in such ribbons, the RBLM phonons are activated due to finite narrow widths and their frequencies are predicted to be inversely proportional to the ribbon widths. In addition, graphene nanoribbons should also exhibit peaks at ∼1450 and 1530 cm^{-1}, corresponding to zigzag and armchair edge phonons, respectively.[33,35] As can be seen in Figure 7, the absence of any peaks at 1450 and 1530 cm^{-1} confirms that our spectral features do not arise from finite width of the graphene sheet. Furthermore, Raman spectra from the same region using a different laser excitation (E_{laser} = 1.96 eV) reveal the RBLMs to be very weakly dispersive unlike the RBMs in SWNTs. Finally, higher order combination Raman modes from this region are very weak in intensity, unlike the corresponding modes in SLG.[24,36]

CONCLUSIONS

We have examined in detail the effect of incommensurate folding in bilayer graphene by analyzing the shift in the G′ band frequency. We show that the contrasting Raman shifts reported for the G′ band frequency in folded single-layer graphene can be rationalized by taking into account the relative strength of fold-induced electron/phonon renormalization.We find that the Raman spectrum of scrolled graphene differs significantly from that of flat graphene. Specifically, we observe an enhanced D band in scrolled graphene due momentum conservation of the intravalley electrons scattered *via* iTO phonons (at the *K*-point) by curvature-induced defect scattering. In addition, we see that the curvature present in the scroll lifts the degeneracy between the LO and TO phonons near the *K*-point and leads to a splitting of the G band into three peaks located at 1570, 1580, and 1592 cm^{-1}. Lastly, the observation of low-frequency radial breathing-like modes confirms that the curvature in the scroll activates new modes that are absent in folded or flat graphene.

METHODS

All samples were prepared using the mechanical exfoliation method as described in ref 25. Raman spectra were acquired with a Dilor XY triple grating and Renishaw InVia Raman microscopes with E_{laser} = 1.96, 2.33, and 2.41 eV. The incident laser beam was focused by a 50× objective, and the laser power on the samples was kept to a minimum to avoid heating. All of the Raman spectra were normalized with respect to the G band intensity and were baseline corrected prior to Lorentzian line shape analysis. Most importantly, the trends in frequency shifts due to folding (*i.e.*, blue, red, or no shift) were the same for both 2.33 and 2.41 eV excitations. Hence, we chose deconvoluted spectra that most clearly reveal the relative shifts between folded and unfolded regions.

Conflict of Interest: The authors declare no competing financial interest.

Acknowledgment. R.R. gratefully acknowledges funding from AFOSR and the National Research Council Postdoctoral Fellowship program. R.T. and M.I. were supported by the National Science Foundation under Grant No. 0955625.

Supporting Information Available: Additional figures and table. This material is available free of charge *via* the Internet at http://pubs.acs.org.

REFERENCES AND NOTES

1. Novoselov, K. S.; Geim, A. K.; Morozov, S. V.; Jiang, D.; Katsnelson, M. I.; Grigorieva, I. V.; Dubonos, S. V.; Firsov, A. A. Two-Dimensional Gas of Massless Dirac Fermions in Graphene. *Nature* **2005**, *438*, 197–200.
2. Lopes dos Santos, J. M. B.; Peres, N. M. R.; Castro-Neto, A. H. Graphene Bilayer with a Twist: Electronic Structure. *Phys. Rev. Lett.* **2007**, *99*, 256802-1–256802-4.
3. Trambly de Laissardiere, G.; Mayou, D.; Magaud, L. Localization of Dirac Electrons in Rotated Graphene Bilayers. *Nano Lett.* **2010**, *10*, 804–808.
4. Shallcross, S.; Sharma, S.; Kandelaki, E.; Pankratov, O. A. Electronic Structure of Turbostratic Graphene. *Phys. Rev. B* **2010**, *81*, 165105–165120.
5. de Heer, W. A.; Berger, C.; Wu, X.; First, P. N.; Conrad, E. H.; Li, X.; Li, T.; Sprinkle, M.; Hass, J.; Sadowski, M. L.; *et al.* Epitaxial Graphene. *Solid State Commun.* **2007**, *143*, 92–100.
6. Schmidt, H.; Luedtke, T.; Barthold, P.; Haug, R. J. Mobilities and Scattering Times in Decoupled Graphene Monolayers. *Phys. Rev. B* **2010**, *81*, 121403–121407.
7. Luican, A.; Li, G.; Reina, A.; Kong, J.; Nair, R. R.; Novoselov, K. S.; Geim, A. K.; Andrei, E. Y. Single-Layer Behavior and Its Breakdown in Twisted Graphene Layers. *Phys. Rev. Lett.* **2011**, *106*, 126802–126806.
8. Sadowski, M. L.; Martinez, G.; Potemski, M.; Berger, C.; de Heer, W. A. Landau Level Spectroscopy of Ultrathin Graphite Layers. *Phys. Rev. Lett.* **2006**, *97*, 266405–266409.
9. Ni, Z.; Wang, Y.; Yu, T.; You, Y.; Shen, Z. Reduction of Fermi Velocity in Folded Graphene Observed by Resonance Raman Spectroscopy. *Phys. Rev. B* **2008**, *77*, 235403–235408.
10. Poncharal, P.; Ayari, A.; Michel, T.; Sauvajol, J. L. Raman Spectra of Misoriented Bilayer Graphene. *Phys. Rev. B* **2008**, *78*, 113407–113411.
11. Sprinkle, M.; Siegel, D.; Hu, Y.; Hicks, J.; Tejeda, A.; Taleb-Ibrahimi, A.; Le Fevre, P.; Bertran, F.; Vizzini, S.; Enriquez, H.; *et al.* First Direct Observation of a Nearly Ideal Graphene Band Structure. *Phys. Rev. Lett.* **2009**, *103*, 226803–226807.
12. Miller, D. L.; Kubista, K. D.; Rutter, G. M.; Ruan, M.; de Heer, W. A.; First, P. N.; Stroscio, J. A. Observing the Quantization of Zero Mass Carriers in Graphene. *Science* **2009**, *324*, 24–927.
13. Fogler, M. M.; Castro Neto, A. H.; Guinea, F. Effect of External Conditions on the Structure of Scrolled Graphene Edges. *Phys. Rev. B* **2010**, *81*, 161408(R)–1611412(R).
14. Braga, S. F.; Coluci, V. R.; Legoas, S. B.; Giro, R.; Galvo, D. S.; Baughman, R. H. Structure and Dynamics of Carbon Nanoscrolls. *Nano Lett.* **2004**, *4*, 881–884.
15. Mpourmpakis, G.; Tylianakis, E.; Froudakis, G. E. Carbon Nanoscrolls: A Promising Material for Hydrogen Storage. *Nano Lett.* **2007**, *7*, 1893–1897.
16. Kim, K.; Lee, Z.; Malone, B. D.; Chan, K. T.; Aleman, B.; Regan, W.; Gannett, W.; Crommie, M. F.; Cohen, M. L.; Zettl, A. Multiply Folded Graphene. *Phys. Rev. B* **2011**, *83*, 245433-1–245433-8.

17. Poncharal, P.; Ayari, A.; Michel, T.; Sauvajol, J. L. Effect of Rotational Stacking Faults on the Raman Spectra of Folded Graphene. *Phys. Rev. B* **2009**, *79*, 195417–195421.
18. Gupta, A. K.; Nisoli, C.; Lammert, P. E.; Crespi, V.; Eklund, P. C. Curvature-Induced D-Band Raman Scattering in Folded Graphene. *J. Phys.: Condens. Matter* **2010**, 334205(1-6).
19. Gupta, A. K.; Tang, Y.; Crespi, V. H.; Eklund, P. C. A Non-dispersive Raman D-Band Activated by Well-Ordered Interlayer Interactions in Rotationally Stacked Bi-Layer Graphene. *Phys. Rev. B* **2010**, *82*, 241406(R)–241410(R).
20. Ferrari, A. C.; Meyer, J. C.; Scardaci, V.; Casiraghi, C.; Lazzeri, M.; Mauri, F.; Piscanec, S.; Jiang, D.; Novoselov, K. S.; Roth, S.; Geim, A. K. Raman Spectrum of Graphene and Graphene Layers. *Phys. Rev. Lett.* **2006**, *97*, 187401–187405.
21. Malard, L.; Pimenta, M.; Dresselhaus, G.; Dresselhaus, M. Raman Spectroscopy in Graphene. *Phys. Rep.* **2009**, *473*, 51–87.
22. Cancado, L. G.; Takai, K.; Enoki, T.; Endo, M.; Kim, Y. A.; Mizusaki, H.; Speziali, N. L.; Jorio, A.; Pimenta, M. A. Measuring the Degree of Stacking Order in Graphite by Raman Spectroscopy. *Carbon* **2008**, *46*, 272–275.
23. Cancado, L. G.; Pimenta, M. A.; Saito, R.; Jorio, A.; Ladeira, L. O.; Grueneis, A.; Souza-Filho, A. G.; Dresselhaus, G.; Dresselhaus, M. S. Stokes and Anti-Stokes Double Resonance Raman Scattering in Two-Dimensional Graphite. *Phys. Rev. B* **2002**, *66*, 035415.
24. Rao, R.; Podila, R.; Tsuchikawa, R.; Katoch, J.; Tishler, D.; Rao, A. M.; Ishigami, M. Effects of Layer Stacking on the Combination Raman Modes in Graphene. *ACS Nano* **2011**, *5*, 1594–1599.
25. Carozo, V.; Almeida, C. M.; Ferreira, E. H. M.; Cancado, L. G.; Achete, C. A.; Jorio, A. Raman Signature of Graphene Superlattices. *Nano Lett.* **2011**, *11*, 4527–4535.
26. Hao, Y.; Wang, Y.; Wang, L.; Ni, Z.; Wang, Z.; Wang, R.; Koo, C. K.; Shen, Z.; Thong, J. T. L. Probing Layer Number and Stacking Order of Few-Layer Graphene by Raman Spectroscopy. *Small* **2010**, *6*, 195–200.
27. Mafra, D. L.; Malard, L. M.; Doorn, S. K.; Htoon, H.; Nilsson, J.; Castro Neto, A. H.; Pimenta, M. A. Observation of the Kohn Anomaly near the K Point of Bilayer Graphene. *Phys. Rev. B* **2009**, *80*, 241414.
28. Maciel, I. O.; Anderson, N.; Pimenta, M. A.; Hartschuh, A.; Qian, H.; Terrones, M.; Terrones, H.; Campos-Delgado, J.; Rao, A. M.; Novotny, L.; *et al.* Electron and Phonon Renormalization near Charged Defects in Carbon Nanotubes. *Nat. Mater.* **2008**, *7*, 878–883.
29. Mohiuddin, T.; Lombardo, A.; Nair, R.; Bonetti, A.; Savini, G.; Jalil, R.; Bonini, N.; Basko, D.; Galiotis, C.; Marzari, N.; *et al.* Uniaxial Strain in Graphene by Raman Spectroscopy: G Peak Splitting, Grüneisen Parameters, and Sample Orientation. *Phys. Rev. B* **2009**, *79*, 205433.
30. Huang, M.; Yan, H.; Chen, C.; Song, D.; Heinz, T. F.; Hone, J. Phonon Softening and Crystallographic Orientation of Strained Graphene Studied by Raman Spectroscopy. *Proc. Natl. Acad. Sci. U.S.A.* **2009**, *106*, 7304–7308.
31. Yang, R.; Shi, Z.; Zhang, L.; Shi, D.; Zhang, G. Observation of Raman G-Peak Split for Graphene Nanoribbons with Hydrogen-Terminated Zigzag Edges. *Nano Lett.* **2011**, *11*, 4083–4088.
32. Zhou, J.; Dong, J. Vibrational Property and Raman Spectrum of Carbon Nanoribbon. *Appl. Phys. Lett.* **2007**, *91*, 173108.
33. Saito, R.; Furukawa, M.; Dresselhaus, G.; Dresselhaus, M. Raman Spectra of Graphene Ribbons. *J. Physics: Condens. Matter* **2010**, *22*, 334203.
34. Vandescuren, M.; Hermet, P.; Meunier, V.; Henrard, L.; Lambin, P. Theoretical Study of the Vibrational Edge Modes in Graphene Nanoribbons. *Phys. Rev. B* **2008**, *78*, 195401.
35. Ren, W.; Saito, R.; Gao, L.; Zheng, F.; Wu, Z.; Liu, B.; Furukawa, M.; Zhao, J.; Chen, Z.; Cheng, H.-M. Edge Phonon State of Mono- and Few-Layer Graphene Nanoribbons Observed by Surface and Interference Co-Enhanced Raman Spectroscopy. *Phys. Rev. B* **2010**, *81*, 035412.
36. Rao, R.; Tishler, D.; Katoch, J.; Ishigami, M. Multiphonon Raman Scattering in Graphene. *Phys. Rev. B* **2011**, *84*, 113406.